

# Lattice Resistance to Dislocation Motion at the Nanoscale

A. Dutta<sup>†</sup>, M. Bhattacharya<sup>‡</sup>, P. Barat<sup>†\*</sup>, P. Mukherjee<sup>‡</sup>, N. Gayathri<sup>‡</sup>, G. C. Das<sup>†</sup>

<sup>†</sup>*School of Materials Science and Technology,  
Jadavpur University, Kolkata 700 032, India*

<sup>‡</sup>*Variable Energy Cyclotron Centre, 1/AF,  
Bidhannagar, Kolkata 700 064, India*

(Dated: October 26, 2018)

## Abstract

In this letter we propose a model that demonstrates the effect of free surface on the lattice resistance experienced by a moving dislocation in nanodimensional systems. This effect manifests in an enhanced velocity of dislocation due to the proximity of the dislocation line to the surface. To verify this finding, molecular dynamics simulations for an edge dislocation in bcc molybdenum are performed and the results are found to be in agreement with the numerical implementations of this model. The reduction in this effect at higher stresses and temperatures, as revealed by the simulations, confirms the role of lattice resistance behind the observed change in the dislocation velocity.

PACS numbers: 61.72.Lk, 62.25.-g

Mechanical properties of crystalline solids are extensively dependent on the dynamics of dislocations in them. This is true even for the nanoscale materials, however, the dynamics is often found to be influenced by the presence of the boundaries, a behavior that is strikingly different from that observed in the bulk [1, 2, 3, 4, 5, 6, 7, 8]. Finite nanoscale systems possess large free surfaces. Thus, the surface plays an important role in the dynamics of dislocation in nanomaterials. The effects of finite length and the termination of a dislocation line at free surfaces have been reported earlier [9, 10]. In addition, many complex phenomena e.g. interaction of dislocation with the surface acoustic waves [11], change in the effective mass of a dislocation near a free surface [12], and drastic rise in the velocity of dislocation near the free surface of a semiconductor presumably due to smaller doping concentration [13] have been intensively studied in the context of surface effects on the dynamics of dislocations. However, the possible role of a free surface in changing the lattice resistance on a dynamic dislocation has not been taken into account to date. A dislocation core near a free surface observes a different surrounding as compared to the one, which is present deep inside the crystal and therefore, is expected to experience a different lattice resistance in its dynamic state. Consequently, it would respond differently under the same loading conditions. Such a variation in the lattice resistance would be reflected in the velocity of dislocation, which would eventually play a fundamental role in the mechanics of materials at low dimensions.

Aiming to explore the possibility of the aforementioned surface effects on moving dislocations, we introduce a model. Using this model we report for the first time, a significant change in the velocity of dislocation due to its proximity to free surfaces when it is moving with its line direction and velocity parallel to the free surfaces. Furthermore, molecular dynamics (MD) simulations have been carried out and the results are found to agree with those obtained from the numerical implementation of this model. In addition, this model exhibits the potential to separate out the lattice resistance from the overall drag experienced by a moving dislocation.

A moving dislocation core passes through periodically varying potential caused by the discreteness of the crystal lattice. The potential gradient opposing the displacement of the core gives rise to the lattice resistance experienced by the dislocation [12, 13]. Our model treats this phenomenon from a novel standpoint. Instead of focusing on the displacement of the moving core of a dislocation explicitly, we concentrate on the dynamic change in the displacement field experienced by the atoms, due to the movement of the dislocation. This

model considers the fact that the potential of an atom in a lattice depends on the atomic configuration of the whole lattice. As a result, a change in the lattice resistance is expected if free surfaces are introduced. On the contrary, other primary drag mechanisms like phonon and electron drags [12, 13, 14] on the moving dislocations are expected to be less sensitive to the presence of the dislocation core in the vicinity of a free surface. Thus, in our model, the net drag force can be split into two components, one of which is strongly influenced by the presence of a dislocation core near a free surface while the other is not. The overall drag coefficient  $B$  and the dislocation velocity  $v$  are related as [13],

$$v(t) = \frac{\tau b}{B}(1 - e^{-Bt/m^*}) \quad (1)$$

where  $\tau$  is the applied shear load,  $b$  is the magnitude of the Burgers vector,  $t$  is the time elapsed after the dislocation starts moving and  $m^*$  is the effective mass per unit length of the dislocation line [12]. The expected change in the drag coefficient  $B$  due to the introduction of the free surfaces leads to the prediction of an altered terminal velocity of dislocation,  $v_0 = \tau b/B$ .

The movement of a dislocation due to the applied force per unit length of the dislocation line ( $\tau b$ ), changes the displacement field felt by the atoms in the lattice. This is resisted by an equal and opposite drag force experienced by the dislocation when it attains its terminal velocity. In the model, we assume that the resistance to any change in the displacement field of an atom due to its interaction with other atoms of the lattice, contributes to the drag force due to the lattice resistance. Cumulative contributions from all the lattice atoms give the overall lattice resistance. Nevertheless, each atom undergoes a different change in the displacement field, and hence should contribute differently to this drag force. Thus, there is need for a contribution function that can express the role of the atoms in determining the net lattice resistance. In order to investigate the surface effects at the nanoscale, a thin film is an ideal system as it provides infinitely large free surfaces with confinement along its thickness.

Consider a dislocation moving with the terminal velocity  $v_0$  along the positive  $x$  direction in a thin film bounded by the top and bottom surfaces in the  $y$  direction. Fig. 1(a) illustrates the configuration of the moving dislocation with the line direction of the dislocation along the  $z$  axis. At an arbitrary time  $t$  the dislocation line passes through the origin O. The

position vector  $\mathbf{r}_{ij}^d(t)$  of the  $ij^{th}$  atom  $A_{ij}$  in the lattice is given by

$$\mathbf{r}_{ij}^d(t) = \mathbf{r}_{ij}^c + \mathbf{u}_{ij}(t, \mathbf{r}_{ij}^c) \quad (2)$$

where  $\mathbf{r}_{ij}^c$  is the position vector of  $A_{ij}$  in the perfect crystal and  $\mathbf{u}_{ij}(t, \mathbf{r}_{ij}^c)$  is the corresponding displacement of the atom in the presence of the dislocation at time  $t$ . In a small time interval  $\delta t$ , the dislocation line proceeds by a distance  $\delta x = v_0 \delta t$  (refer Fig. 1(b)). The net force due to the lattice resistance is given by

$$F_s^{(lattice)} = \sum_{i=s_1}^{s_2} \sum_{j=-\infty}^{\infty} \phi_{ij}, \quad (3)$$

where  $\phi_{ij}$  denotes the contribution of the atom  $A_{ij}$  to the lattice resistance. We assume a simple proportionality relation between  $\phi_{ij}$  and the change in the position vector of  $A_{ij}$  in time  $\delta t$  as

$$\phi_{ij} = \kappa \left| \mathbf{r}_{ij}^d(t + \delta t) - \mathbf{r}_{ij}^d(t) \right|, \quad (4)$$

where  $\kappa$  is the proportionality constant for a given loading condition. In terms of  $\delta t$  as the unit of time,

$$F_s^{(lattice)} = B_s^{(lattice)} v_0, \quad (5)$$

where

$$B_s^{(lattice)} = \kappa \sum_{i=s_1}^{s_2} \sum_{j=-\infty}^{\infty} \left| \sum_{n=1}^{\infty} \frac{v_0^{n-1}}{n!} \left( \frac{\partial^n \mathbf{u}_{ij}}{\partial (\delta x)^n} \right)_{\delta x=0} \right|. \quad (6)$$

A different value of the drag coefficient  $B_s^{(lattice)}$  is quite obvious following Eq. (6) due to the change in the summation limits of  $i$  representing the thickness of the film. A reduction in the lattice resistance for a thinner film is indicative of an enhanced velocity of dislocation. Similar changes are expected due to the variation in position of the dislocation line along the film thickness. MD simulations are carried out to verify such effects.

A typical simulation starts with a virtual freestanding thin film of single crystal bcc molybdenum created using the Finnis-Sinclair potential [15]. The simulation cell is shown in Fig. 2 with its  $x$ ,  $y$  and  $z$  axes along  $\langle 111 \rangle$ ,  $\langle \bar{1}01 \rangle$ , and  $\langle 1\bar{2}1 \rangle$  directions respectively. The crystal dimensions along the  $x$  and  $z$  Cartesian directions are 10.76 nm and 3.85 nm respectively, whereas the  $y$  dimension representing the film thickness is varied to study the surface and size effects. An edge dislocation is introduced at the centre of the film with

dislocation line along the  $z$  axis and Burgers vector  $a\langle 111 \rangle/2$  along the  $x$  direction where the lattice constant  $a=0.31472$  nm. Periodic boundary conditions are imposed on all the three directions, however, the boundaries are sufficiently extended along the  $y$  direction so that free top and bottom surfaces can be created and interactions among the periodic image films can be eliminated. The dislocation core is identified by specifying a centrosymmetric deviation parameter window [16] of width 0.024-0.1 nm<sup>2</sup>. The system is then initialized at 300 K temperature. Precisely calculated forces are applied to the atoms of the top and bottom surfaces of the film with directions parallel and antiparallel to the Burgers vector respectively so that a shear stress of 250 MPa can be produced. Following a time lag, this applied stress is transmitted to the dislocation line, which in turn attains a terminal velocity in several femtoseconds [16] following Eqn. (1). Constant temperature is maintained by implementing the Nosé-Hoover thermostat [17, 18]. Trajectories of all the atoms are calculated at a time step of 0.5 fs. Positions of the dislocation core are recorded with respect to time and thus the dislocation velocity is extracted. Simulations are performed in two ways, case I: by reducing the film thickness equally about the dislocation line and case II: by varying the position of the dislocation line at different depths beneath the top surface of a film of fixed thickness.

Figure 3(a) shows the variation in the velocity of edge dislocation as a function of film thickness. The MD simulations clearly exhibit a significant increase in this velocity when the film thickness is reduced from  $\sim 70$  nm to 8.5 nm. However, at higher thicknesses the velocity of dislocation attains a constant value of  $\sim 728$  m/sec. A significant rise of 46% in this velocity for the film of 8.5 nm thickness under the same loading conditions is noteworthy in this context. A rising trend in the dislocation velocity is also observed as the dislocation line is brought closer to the top free surface in a film of 35.2 nm thickness (refer Fig. 3(b)).

The results obtained from the MD simulations establish the effects of surface and size on the velocities of dislocations in thin films. These results have been used as a tool to separate out the contribution of lattice resistance from the overall drag. Equation (5) enables us to express the net drag coefficient  $B$  as the sum of the drag coefficients due to lattice resistance  $B_s^{(lattice)}$  and the remaining part  $B'$  due to other drags.  $B$  values are calculated using the velocities of dislocation extracted from MD simulations for two widely different film thicknesses. The ratio of the drag coefficients corresponding to the lattice resistance for these two film thicknesses is evaluated and then used to separate out the constant part  $B'$

from  $B$ . The net drag coefficient  $B$  for any arbitrary film thickness is obtained by combining the calculated values of  $B'$  and  $B_s^{(lattice)}$  so that the respective velocity of dislocation can be evaluated. In order to perform these calculations, the position vectors of the atoms are determined by superposing the following elastic displacement fields of an edge dislocation [12] on a perfect bcc crystal;

$$u_x(x, y) = \frac{b}{2\pi} \left[ \tan^{-1} \frac{y}{x} + \frac{xy}{2(1-\nu)(x^2 + y^2)} \right], \quad (7)$$

$$u_y(x, y) = -\frac{b}{2\pi} \left[ \frac{1-2\nu}{4(1-\nu)} \ln(x^2 + y^2) + \frac{x^2 - y^2}{4(1-\nu)(x^2 + y^2)} \right], \quad (8)$$

$$u_z(x, y) = 0, \quad (9)$$

where the value of the Poisson's ratio  $\nu$  is 0.3 [19]. The change in the displacement fields of atoms due to the incremental change  $\delta x$  in the dislocation line position can be found to decay rapidly with the distance from the dislocation line as compared to the displacement field itself. Hence, the interactions among the periodic image dislocations are not expected to affect the results significantly. Thus, the numerical computations have been done taking into account 200 atoms on both sides of the dislocation line in each row along the  $x$  direction. Number of rows and the position of the origin are varied according to the configurations in case I and case II respectively. The results of the calculations are shown in Fig. 3(a) and (b) in the form of solid lines. The model is found to reproduce the trends observed in MD simulations.

Dislocation velocity at applied shear stress  $\tau$  and temperature  $T$  is empirically given as  $v \sim \tau^m \exp(-Q/kT)$  where  $m$  is the stress exponent [13, 20]. However, with rise in stress and temperature, the phonon drag becomes the predominant mechanism governing the dynamics of dislocations [21]. Since this phonon drag primarily constitutes  $B'$ , the size effect on the velocity of dislocation should diminish at higher temperatures and applied stresses. Figure 4 represents the velocities of the edge dislocation obtained from the MD simulations for

three different film thicknesses at three different applied loads as a function of temperature. The size effect on this velocity is noticeable only at 250 MPa shear stress and disappears at higher stresses of 500 MPa and 1000 MPa for the entire range of temperature studied. The MD simulations performed at 250 MPa stress show a decrease in the velocity of dislocation with increasing temperature. The reduction in the dispersion of the velocity of dislocation with thicknesses of thin films at higher stresses and temperatures is supportive of the fact that lattice resistance is the key factor behind the observation of the effects under discussion.

This letter reports a pronounced change in the velocity of a dislocation due to the presence of a free surface in the proximity of the dislocation line in a finite nanoscale crystalline solid. This effect has been attributed to the altered lattice resistance in different system configurations. A model following an unconventional approach to the lattice resistance has been developed that serves as a tool for explaining these observations. The fundamental ideas as well as the proposed model have been verified through the MD simulations of an edge dislocation in bcc molybdenum. Similar studies are yet to be done for more complex types of dislocations in different crystal structures and this largely simplified model provides ample scope of necessary modifications to suite these special cases. Development of a generalized model, especially the one covering up to the bulk regime needs further intensive study where the ideas as presented here, can provide a fundamental framework for the understanding of the mechanism of the lattice resistance along with the associated dislocation dynamics.

The authors thank Dr. Wei Cai for technical suggestions regarding the use of the MD++ molecular dynamics package.

- 
- [1] Steffen Brinckmann, Ju-Young Kim, and Julia R. Greer, *Phys. Rev. Lett.* **100**, 155502 (2008).
  - [2] A. K. Schmid, N. C. Bartelt, J. C. Hamilton, C. B. Carter, and R. Q. Hwang, *Phys. Rev. Lett.* **78**, 3507 (1997).
  - [3] L. Nicola, E. Van der Giessen, and A. Needleman, *J. Appl. Phys.* **93**, 5920 (2003); L. Nicola, E. Van der Giessen, and A. Needleman, *Thin Solid Films* **479**, 329 (2005).
  - [4] H. Tang, K. W. Schwarz, and H. D. Espinosa, *Phys. Rev. Lett.* **100**, 185503 (2008).
  - [5] K. A. Afanasyev and F. Sansoz, *Nano Lett.* **7**, 2056 (2007).

- [6] Julia R. Greer and William D. Nix, Phys. Rev B **73**, 245410 (2006).
- [7] M. Yu. Gutkin, I. A. Ovid'ko, and N. V. Skiba, Phys. Rev. B **74**, 172107 (2006).
- [8] L. B. Freund and S. Suresh, *Thin Film Materials* (Cambridge University press, Cambridge, England, 2006).
- [9] Karin Lin, and D. C. Chrzan, Phys. Rev. B **60**, 3799 (1999).
- [10] E. Bitzek and P. Gumbsch, Mater. Sci. Engg. A **387-389**,11 (2004).
- [11] A. Maurel, V. Pagneux, F. Barra, and F. Lund, Phys. Rev. B **75**, 224112 (2007).
- [12] J. P. Hirth and J. Lothe, *Theory of Dislocations* (John Wiley and Sons., New York, 1982).
- [13] E. Nadgorny, Progr. Mater. Sci. **31**, 1 (1988).
- [14] V. I. Alshits and V. L. Indenbom, in *Dislocations in Solids*, edited by F. R. N. Nabarro (North-Holland, New York, 1986), Chap 34.
- [15] M. W. Finnis and J. E. Sinclair, Phil. Mag. **50**, 45 (1984).
- [16] V. V. Bulatov and W. Cai, *Computer Simulations of Dislocations* (Oxford University Press, Oxford, 2006).
- [17] S. Nosé, Mol. Phys. **52**, 255 (1984).
- [18] W. G. Hoover, Phys. Rev. A **31**, 1695 (1985).
- [19] D. C. Hurley, V. K. Tewary, and A. J. Richards, Thin Solid Films **398-399**, 326 (2001).
- [20] W. Cai, V. V. Bulatov, J. Chang, J. Li and S. Yip, in *Dislocations in Solids*, edited by F. R. N. Nabarro and J. P. Hirth (North-Holland, New York, 2004), Chap 64.
- [21] J. Chang, W. Cai, V. V. Bulatov, and S. Yip, Mater. Sci. Engg. A **309-310**, 160 (2001).

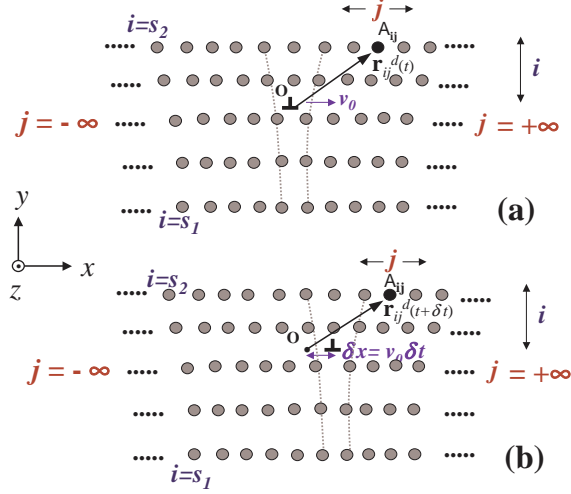


FIG. 1: Schematic representation of the model. (a) The edge dislocation line is along the  $z$  axis and is at the origin  $O$  at time  $t$ . A thin film is confined in  $y$ -dimension, where  $i = s_1$  and  $i = s_2$  are the free surfaces. The dislocation is moving with terminal velocity  $v_0$  along the positive  $x$  direction.  $\mathbf{r}_{ij}^d(t)$  is the position vector of the  $ij^{th}$  atom  $A_{ij}$ . (b) In time  $\delta t$ , the dislocation moves through  $\delta x$  towards the positive  $x$  direction and  $\mathbf{r}_{ij}^d(t + \delta t)$  is the position vector of the atom  $A_{ij}$  at time  $t + \delta t$ .

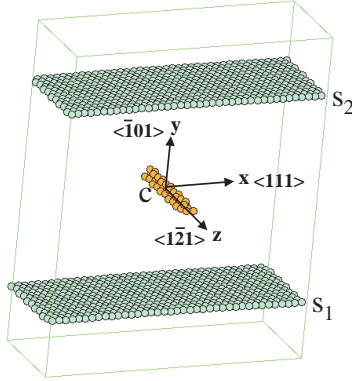


FIG. 2: The MD simulation cell with the indicated crystal directions. Only the atoms at surfaces ( $s_1, s_2$ ) and the edge dislocation core (C) are displayed for clarity. Here the boundaries are extended along the  $y$  direction.

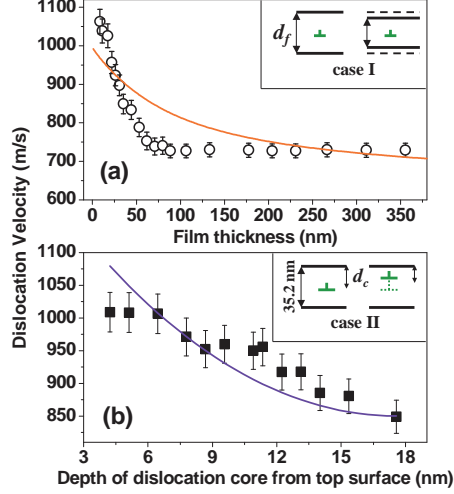


FIG. 3: (color online). (a) The dislocation velocity obtained from MD simulations is plotted (circles) as a function of film thickness  $d_f$  (case I). Here the dislocation line is equidistant from both the free surfaces of the film as illustrated schematically in the inset. (b) The dislocation velocity extracted from MD simulations is presented (squares) for different depths of the dislocation line from the top surface ( $d_c$ ) of the film of 35.2 nm thickness (see case II in the inset). The solid lines represent the output of numerical calculations based on the model in both (a) and (b). Shear stress and temperature are 250 MPa and 300 K respectively. Error bars for MD simulation results as indicated in both the plots are due to the randomness of the initial velocities and positions of the atoms in the simulation cell.

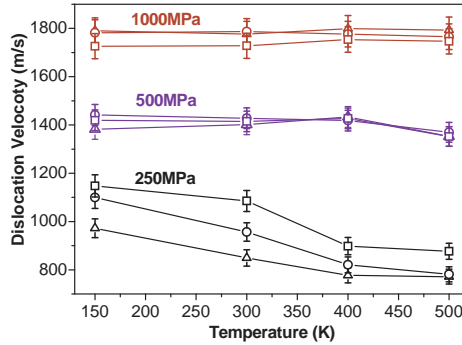


FIG. 4: (color online). Variation of the dislocation velocities with temperature is plotted for three different film thicknesses 8.5 nm (square), 21.8 nm (circle) and 35.2 nm (triangle) at three different shear stresses of 250 MPa, 500 MPa and 1000 MPa. Error bars are indicated in the figure. The dispersion of dislocation velocity with film thickness reduces at higher temperature and stresses.